change of enzyme.

The degree of activation observed with a synthetic cofactor, (6*RS*)-6-methyltetrahydropterin, was less than that with the natural cofactor, (6*R*)-L-*erythro*-tetrahydrobiopterin. Similar results are reported upon activation by phenylalanine (Kaufman & Mason, 1982), phosphorylation (Abita et al., 1976), limited proteolysis (Abita et al., 1984), or chemical modification (Parniak & Kaufman, 1981).

It is not known if phenylalanine hydroxylase is regulated via modification of SH residues in vivo. Since the disulfide formation is likely to occur in vivo, SH groups could have a regulatory role in the activation of phenylalanine hydroxylase in vivo. Furthermore, the stabilization against the thermal denaturation with reagent **3** indicates the possibility of producing a stable enzyme preparation by chemical modification.

In conclusion, a new family of asymmetric thiol–disulfide exchange reagents, DNPSSR, were shown to have considerable potential as active site probes. The reagents were used to further characterize the activation of phenylalanine hydroxylase by SH modification.

ACKNOWLEDGMENTS

We are grateful to Dr. Gordon Guroff (National Institutes of Health, Bethesda, MD) for his kind help in the preparation of the manuscript.

REFERENCES

Abita, J. P., Milstien, S., Chang, N., & Kaufman, S. (1976) *J. Biol. Chem. 251*, 5310–5314.

Baily, S. W., & Ayling, J. E. (1980) *Anal. Biochem. 107*, 156–164.

Fisher, D. B., & Kaufman, S. (1973) *J. Biol. Chem. 248*, 4345–4353.

Kaufman, S. (1959) *J. Biol. Chem. 234*, 2677–2682.

Kaufman, S. (1971) *Adv. Enzymol. Relat. Areas Mol. Biol. 35*, 245–319.

Kaufman, S., & Mason, K. (1982) *J. Biol. Chem. 257*, 14667–14678.

Laemmli, U. K. (1970) *Nature (London) 227*, 680–685.

Matsuura, S., Murata, S., & Sugimioto, T. (1985) *J. Biochem. (Tokyo) 23*, 3115–3120.

Motion, R. L., Blackwell, L. F., & Buckley, P. D. (1984) *Biochemistry 23*, 6852–6857.

Parker, A. J., & Kharasch, N. (1960) *J. Am. Chem. Soc. 82*, 3071–3075.

Parniak, M. A., & Kaufman, S. (1981) *J. Biol. Chem. 256*, 6876–6882.

Rao, D. N., & Kaufman, S. (1986) *J. Biol. Chem. 261*, 8866–8876.

Scriver, C. R., & Clow, C. L. (1980) *Annu. Rev. Genet. 14*, 179–202.

Sekine, T., Barnett, L. M., & Kielley, W. W. (1962) *J. Biol. Chem. 237*, 2796–2772.

Sekine, T., Takahashi, S., Hikita, S., Sutoh, N., & Satake, K. (1984) *J. Biochem. (Tokyo) 96*, 27–33.

Shiman, R., & Gray, D. W. (1980) *J. Biol. Chem. 255*, 4793–4800.

Shiman, R., Gray, D. W., & Peter, A. (1979) *J. Biol. Chem. 254*, 11300–11306.

Wilkinson, G. N. (1961) *Biochem. J. 80*, 324–332.

Determination of the Energetics of the UDP-glucose Pyrophosphorylase Reaction by Positional Isotope Exchange Inhibition†

Leisha S. Hester and Frank M. Raushel*

Departments of Chemistry and Biochemistry, Texas A&M University, College Station, Texas 77843

Received April 10, 1987

ABSTRACT: A method has been developed for obtaining qualitative information about enzyme-catalyzed reactions by measuring the inhibitory effects of added substrates on positional isotope exchange rates. It has been demonstrated for ordered kinetic mechanisms that an increase in the concentration of the second substrate to add to the enzyme will result in a linear increase in the ratio of the chemical and positional isotope exchange rates. The slopes and intercepts from these plots can be used to determine the partitioning ratios of binary and ternary enzyme complexes. The method has been applied to the reaction catalyzed by UDP-glucose pyrophosphorylase. A positional isotope exchange reaction was measured within oxygen-18-labeled UTP as a function of variable glucose 1-phosphate concentration in the forward reaction. In the reverse reaction, a positional isotope exchange reaction was measured within oxygen-18-labeled UDP-glucose as a function of increasing pyrophosphate concentration. The results have been interpreted to indicate that the interconversion of the ternary central complexes is fast relative to product dissociation in either direction. In the forward direction, the release of UDP-glucose is slower than the release of pyrophosphate. The release of glucose 1-phosphate is slower than the release of UTP in the reverse reaction.

The positional isotope exchange (PIX)[1] technique, first developed by Midelfort and Rose (1976), has become a widely used technique in mechanistic enzymology. The technique can be applied to any enzyme system in which functionally nonequivalent groups become torsionally equivalent via a reaction intermediate or product, thus allowing scrambling of isotopically labeled substituents within a substrate. Traditionally,

† This work was supported by the National Institutes of Health (GM-33874) and the Robert A. Welch Foundation (A-840). F.M.R. is the recipient of NIH Research Career Development Award DK-01366. The authors acknowledge with thanks financial support by the Board of Regents of Texas A&M University.

* Address correspondence to this author at the Department of Chemistry, Texas A&M University.

[1] Abbreviations: HPLC, high-performance liquid chromatography; PIX(E), positional isotope exchange (enhancement); HEPES, *N*-(2-hydroxyethyl)piperazine-*N*′-2-ethanesulfonic acid; MES, 2-(*N*-morpholino)ethanesulfonate; EDTA, ethylenediaminetetraacetic acid; Tris, tris(hydroxymethyl)aminomethane.

0006-2960/87/0426-6465$01.50/0

the PIX technique has been used to determine the kinetic competence of proposed intermediates in enzyme-catalyzed systems (von der Saal et al., 1985; Raushel & Villafranca, 1980; DeBrosse & Villafranca, 1983; Hasset et al., 1982). More recently, Raushel and Garrard (1984) showed that a PIX investigation of the argininosuccinate lyase reaction could be used to probe the reaction flux through alternate pathways in enzyme mechanisms. These results broadened the utility of the PIX technique by permitting the determination of the relative rates of release of the two products from the enzyme–product complex.

In the study of enzyme reaction mechanisms, it is of interest to determine the individual rate constants for the interconversion of all enzyme complexes. However, the complete solution to all of the microscopic rate constants in an enzyme-catalyzed reaction has been achieved only rarely (Albery & Knowles, 1976, 1986). It would therefore be advantageous to have additional kinetic techniques that could determine the overall kinetic mechanism and measure the partitioning of the enzyme complexes and, more importantly, the individual rate constants. Toward this end, we have derived the equations for the effects of added substrates on the ratio of the PIX and chemical rates in ordered kinetic mechanisms. This new application of the PIX technique complements the PIXE technique of Raushel and Garrard (1984) wherein the effects of added products were used to enhance the rate of the PIX reaction relative to the net formation of products. This new methodology has also been applied to the UDP-glucose pyrophosphorylase reaction.

UDP-glucose pyrophosphorylase catalyzes the transfer of the uridylyl group from UTP to glucose 1-phosphate to form UDP-glucose and pyrophosphate:

$$\text{UTP} + \text{glucose 1-phosphate} \rightleftharpoons \text{PP}_i + \text{UDP-glucose} \quad (1)$$

Tsuboi et al. (1969) determined the kinetic mechanism to be sequential Bi-Bi ordered with UTP binding first and UDP-glucose the last product released. The stereochemistry of the UDP-glucose pyrophosphorylase reaction proceeds by net inversion of configuration at the α-phosphorus of UTP (Shue & Frey, 1979). Therefore, the reaction proceeds by the direct transfer of the uridylyl group from UTP to glucose 1-phosphate.

A different PIX reaction can be studied in both the forward and reverse directions of the UDP-glucose pyrophosphorylase reaction. These two reactions are shown in eq 2 and 3, respectively. In the forward reaction, [β-$^{18}O_2$,$\beta\gamma$-^{18}O,γ-$^{18}O_3$]UTP (I) is used as the substrate. In the presence of glucose 1-phosphate, the enzyme catalyzes the cleavage of the bond between the α-phosphorus of UTP and the α,β-bridging oxygen. The potential torsional scrambling of the β-phosphoryl group of the resulting PP_i would result in the formation of [$\alpha\beta$-^{18}O,β-^{18}O,$\beta\gamma$-^{18}O,γ-$^{18}O_3$]UTP (II) upon re-formation of the initial substrates. The equilibration of I and II can be detected by ^{31}P NMR spectroscopy as described by Cohn and Hu (1980). In the reverse reaction, [β-$^{18}O_3$]UDP-glucose can be used as the PIX substrate. In the presence of PP_i, the bond between the α-phosphorus and the α,β-bridging oxygen of UDP-glucose is broken. Rotation of the phosphoryl group of glucose 1-phosphate would then result in the equilibration of III and IV upon re-formation of UDP-glucose. This PIX reaction can also be monitored by ^{31}P NMR spectroscopy.

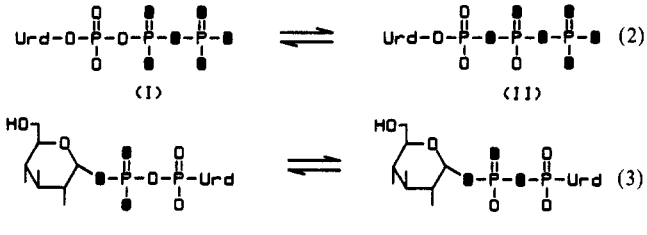

(2)

(3)

Materials and Methods

Sucrose synthetase was isolated from wheat germ according to the procedure of Singh et al. (1987). Oxygen-18-labeled potassium phosphate was made according to the procedure of Risley and Van Etten (1978). Oxygen-18-labeled water (97%) was purchased from Cambridge Isotope Laboratories. All other reagents were purchased from Sigma.

Preparation of [β-$^{18}O_2$,$\beta\gamma$-^{18}O,γ-$^{18}O_3$]*UTP (I).* UTP labeled with six atoms of oxygen-18 at the β- and γ-phosphoryl groups was synthesized enzymatically with carbamate kinase, nucleoside-monophosphate kinase, and nucleoside-diphosphate kinase. Carbamyl [$^{18}O_4$]phosphate was synthesized according to the procedure of Cohn and Hu (1980). The UTP synthesis reaction mixture contained 10 mM UMP, 7.5 mM ADP, 50 mM HEPES, pH 7.5, 20 mM $MgCl_2$, 25 mM carbamyl [$^{18}O_4$]phosphate, 50 units of carbamate kinase, 12 units of nucleoside-monophosphate kinase, and 25 units of nucleoside-diphosphate kinase in a volume of 100 mL. The reaction was monitored by HPLC using a Whatman SAX anion-exchange column. After 150 min, the reaction was quenched by lowering the pH to 3.0. Carbamate kinase, nucleoside-monophosphate kinase, and nucleoside-diphosphate kinase were removed by passage of the sample through a YM-30 ultrafiltration membrane (Amicon). The nucleotides were separated by passage through a Whatman DE-52 anion-exchange column. The eluting buffer was a 2.0-L gradient of 10–500 mM triethylamine bicarbonate, pH 7.5. The yield was 700 μmol of labeled UTP.

Preparation of [β-$^{18}O_3$]*UDP-glucose (III).* UDP-glucose labeled with oxygen-18 at the β-phosphoryl group was synthesized enzymatically with carbamate kinase, nucleoside-monophosphate kinase, and sucrose synthetase in two steps. The first step involved the formation of [β-$^{18}O_3$]UDP, and the second step involved the formation of [β-$^{18}O_3$]UDP-glucose. The first reaction mixture contained 10 mM UMP, 7.5 mM ADP, 50 mM HEPES, pH 7.5, 20 mM $MgCl_2$, 10 mM carbamyl [$^{18}O_4$]phosphate, 50 units of carbamate kinase, and 12 units of nucleoside-monophosphate kinase in a volume of 100 mL. After 100 min, the reaction was quenched by lowering the pH to 3.0, and then the carbamate kinase and nucleoside-monophosphate kinase were removed by passage of the sample through a YM-30 ultrafiltration membrane (Amicon). The nucleotides were separated by passage through a Whatman DE-52 anion-exchange column. The eluting buffer was a 2.0-L gradient of 10–250 mM triethylamine bicarbonate, pH 7.5. [β-$^{18}O_3$]UDP was isolated (500 μmol) and used in the synthesis of [β-$^{18}O_3$]UDP-glucose. The reaction mixture contained 10 mM [β-$^{18}O_3$]UDP, 50 mM sucrose, 25 mM MES, pH 6.0, and 6.0 units of sucrose synthetase in a volume of 50 mL. The reaction was quenched, and the product was isolated by chromatography on DE-52. The yield was 400 μmol of [β-$^{18}O_3$]UDP-glucose.

^{31}P Nuclear Magnetic Resonance Measurements. ^{31}P NMR spectra were obtained on a Varian XL-400 multinuclear spectrometer operating at a frequency of 162 MHz. Typical acquisition parameters were 6000-Hz sweep width, 2.5-s acquisition time, no delay between pulses, 15-μs pulse width (pulse width 90° = 25 μs), and Waltz decoupling (4 dB). All spectra were internally referenced to phosphate, pH 9.0.

Positional Isotope Exchange. In the forward direction, the positional isotope exchange reaction was followed by moni-

toring the interchange of the α,β-bridge and β-nonbridge oxygens of UTP (see eq 2). The reaction conditions were 5 μmol of [β,γ-$^{18}O_6$]UTP, 10 μmol of glucose-1-P, 1.0 mM $MgCl_2$, 50 mM HEPES, pH 7.5, 1 unit/mL inorganic pyrophosphatase, and an appropriate amount of UDP-glucose pyrophosphorylase. The volumes of the individual assays were adjusted to obtain the final concentration of glucose-1-P which ranged from 0.01 to 1.0 mM. After the reaction had reached 40–60% completion as monitored by HPLC, the reaction was terminated by the addition of carbon tetrachloride, vigorous vortexing, and lowering of the pH to 4. After centrifugation, the pH of the sample was raised to 8.0 and the sample applied to a DE-52 anion-exchange column. The UTP was eluted with an 800-mL gradient of 10–500 mM triethylamine bicarbonate buffer, pH 7.5. The pooled fractions containing the [$^{18}O_6$]UTP were dried by rotary evaporation and washed with methanol. The sample was then dissolved in 3 mL of a solution containing 100 mM EDTA, 50 mM P_i, 150 mM Tris, pH 9, and 25% D_2O and stored frozen.

The positional isotope exchange reaction in the reverse direction was monitored by following the interchange of the β-nonbridge oxygens with the α,β-bridge oxygen of [β-$^{18}O_3$]UDP-glucose. The reaction conditions were 10 μmol of [β-$^{18}O_3$]UDP-glucose, 20 μmol of pyrophosphate, 20 μmol of NADP, 3 mM $MgCl_2$, 0.5 mM cysteine, 5 μM glucose 1,6-bisphosphate, 25 mM HEPES, pH 7.5, 1 unit/mL phosphoglucomutase, and 1 unit/mL glucose-6-phosphate dehydrogenase. The final volume of the reaction mixture was varied to give the desired concentration of pyrophosphate (0.05–2.0 mM). Approximately 0.5 unit of UDP-glucose pyrophosphorylase was added to initiate the reaction. The reaction was monitored at 340 nm until the reaction reached 50%. The reaction was terminated by lowering the pH to 3.5, and the enzymes were removed by passage through a YM-30 ultrafiltration membrane (Amicon). The [β-$^{18}O_3$]UDP-glucose was purified by chromatography on a column of DE-52.

The rate constants for the positional isotope exchange were calculated from the equation of Litwin and Wimmer (1979):

$$v_{ex} = \left(\frac{X}{\ln (1 - X)}\right)\left(\frac{A_0}{t}\right) \ln (1 - F) \qquad (4)$$

where X = the fractional change of the original nucleotide (UTP or UDP-Glc) pool, F = the fraction of equilibrium value obtained at time t, and A_0 = the concentration of the original nucleotide pool.

Enzyme Assays. Enzyme assays and absorbance measurements were made with a Gilford 260 UV–vis spectrophotometer and a Linear 255 recorder. The kinetic data were fit to the Fortran programs of Cleland (1967) that have been translated into BASIC.

Initial Rate Measurements. Enzyme activity in the forward direction was measured spectrophotometrically at 340 nm. Each cuvette contained 3 mM $MgCl_2$, 25 mM HEPES, pH 7.5, 0.5 mM NAD, and 0.05 unit of UDP-glucose dehydrogenase. In the determination of the K_m for UTP, glucose-1-P concentration was held at 0.5 mM while UTP concentration was varied. When glucose-1-P concentration was varied, the UTP concentration was held at 1.0 mM. The kinetics in the reverse direction were determined by monitoring the formation of glucose-1-P. Each 3-mL cuvette contained 2 mM cysteine, 25 mM HEPES, pH 7.5, 2 mM $MgCl_2$, 1 μM glucose 1,6-bisphosphate, 0.5 mM NAD, 3 units of phosphoglucomutase, and 3 units of glucose-6-phosphate dehydrogenase. Pyrophosphate concentration was held at 0.5 mM while UDP-glucose concentration was varied, and UDP-glucose concentration was held at 3 mM while pyrophosphate concentration was varied.

Scheme I

$$E \underset{k_2}{\overset{k_1A}{\rightleftharpoons}} EA \underset{k_4}{\overset{k_3B}{\rightleftharpoons}} EAB \underset{k_6}{\overset{k_5}{\rightleftharpoons}} EPQ \underset{k_8P}{\overset{k_7}{\rightleftharpoons}} EQ \underset{k_{10}Q}{\overset{k_9}{\rightleftharpoons}} E$$

Determination of the Bound Equilibrium Constant. The equilibrium constant for the interconversion of bound products and substrates was measured by incubation of the enzyme with a fixed amount of either UDP-glucose or UTP and various concentrations of a 1:1 mixture of PP_i and glucose-1-P. From the UTP direction, each 0.05-mL incubation mixture contained 20 μM UTP, 5 mM Mg^{2+}, 50 mM HEPES, pH 7.5, and 50 units of UDP-glucose pyrophosphorylase. The concentration of PP_i/glucose-1-P was varied from 0.5 to 3 mM. The reaction was quenched by lowering the pH of the reaction mixture to 2.5 with phosphoric acid. The concentration of UTP was then quantitated by HPLC. From the UDP-glucose direction, each 0.05-mL incubation mixture contained 17 μM UDP-glucose in addition to the other components as indicated above. After being quenched with phosphoric acid, the UTP that was formed was quantitated by HPLC.

THEORY

The simplest general mechanism that can be written for the UDP-glucose pyrophosphorylase reaction is shown in Scheme I where A = UTP, B = glucose 1-phosphate, P = pyrophosphate, and Q = UDP-glucose. The chemistry occurs between EAB and EPQ. The partitioning of the EAB and EPQ complexes during the steady state can be determined by measuring the positional isotope exchange rates relative to the net product formation in either the forward or the reverse reaction (v_{chem}/v_{ex}). In the forward direction, the step for the addition of PP_i can be neglected because excess inorganic pyrophosphatase will keep the concentration of PP_i essentially zero. The partitioning of the EPQ complex can then be written in terms of the individual rate constants using the theory of net rate constants of Cleland (1975). The partitioning of EPQ can then be presented as

$$\frac{v_{chem}}{v_{ex}} = \frac{k_7[EPQ]}{k_6'[EPQ]} = \frac{k_7(k_2k_4 + k_2k_5 + k_3k_5[B])}{k_2k_4k_6} \qquad (5)$$

The partitioning of EPQ is therefore directly proportional to the concentration of B, and thus a plot of v_{chem}/v_{ex} vs. [B] is linear. The PIX rate goes to zero at saturating levels of B. The expression for the ratio of rates at zero B (R_1) is shown in eq 6, and the concentration of B that increases this value by a factor of 2 (B_x) is shown in eq 7. If the order of addition

$$R_1 = k_7(k_4 + k_5)/k_4k_6 \qquad (6)$$

$$B_x = k_2(k_4 + k_5)/k_3k_5 \qquad (7)$$

of the two substrates had been reversed (glucose-1-P adds before UTP), then there would be no effect on the exchange ratio by changing the concentration of B (glucose-1-P). This is because the binding of the first substrate to the enzyme cannot influence the dissociation rate of the second substrate that binds to the enzyme. If the addition of the substrates is random, the plot of v_{chem}/v_{ex} vs. [B] will plateau at a value of v_{chem}/v_{ex} that equals the flux through the alternate pathway.

Analogous equations can also be derived for similar experiments initiated in the reverse direction with labeled UDP-glucose. The step for addition of glucose-1-P (k_3) can be neglected because excess phosphoglucomutase and glucose-6-P dehydrogenase will rapidly reduce the concentration

Scheme II

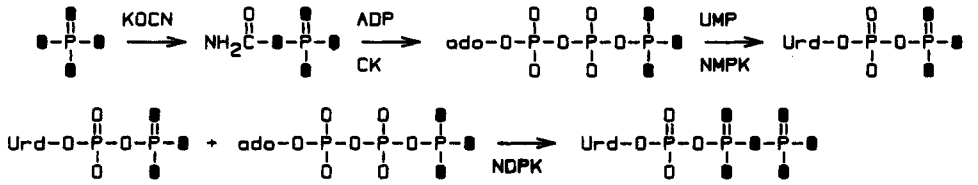

of glucose-1-P to zero. The value for the ratio of rates at zero P (R_2) is

$$R_2 = k_4(k_6 + k_7)/k_5k_7 \quad (8)$$

and the concentration of P that increases this value by a factor of 2 (P_x) is

$$P_x = k_9(k_6 + k_7)/k_6k_8 \quad (9)$$

Results

The strategy for preparing oxygen-18-labeled UTP (I) is shown in Scheme II. The synthesis starts with the preparation of [γ-$^{18}O_3$]ATP as catalyzed by carbamate kinase in the presence of ADP and oxygen-18-labeled carbamyl phosphate. The γ-phosphoryl group of ATP is then transferred to UMP by the action of nucleoside-monophosphate kinase and finally to the labeled UDP by nucleoside-diphosphate kinase. The ^{31}P NMR spectrum of the oxygen-18-labeled UTP (I) is shown in Figure 1A. Integration of the separate resonances for the γ-phosphoryl group in which two, three, and four atoms of oxygen-18 are directly bonded to the γ-phosphate indicates that the overall incorporation of oxygen-18 into the β- and γ-phosphoryl groups is 90%.

The high level of oxygen-18 incorporation into only the β- and γ-phosphoryl groups is confirmed by mixing unlabeled UTP with the labeled UTP as shown in the NMR spectrum presented in Figure 1B. As expected, the α-phosphoryl group is completely devoid of oxygen-18. The upfield isotopic chemical shift induced by the four oxygen-18 atoms directly bonded to the γ-P is 0.089 ppm (0.022/atom). The three atoms of oxygen-18 directly bonded to the β-phosphoryl group induce a 0.073 ppm upfield isotopic chemical shift. The two β-nonbridge oxygen-18 atoms each contribute a 0.029 ppm upfield shift while the β,γ-bridge oxygen-18 induces a shift of 0.014 ppm. Similar shifts have been obtained for ATP (Cohn, 1982).

UDP-glucose pyrophosphorylase catalyzes the exchange of a β-nonbridge oxygen-18 with the unlabeled α,β-bridge position within [β-$^{18}O_2$,$\beta\gamma$-^{18}O,γ-$^{18}O_3$]UTP only in the presence of glucose-1-P. The ^{31}P NMR spectrum (Figure 1C) of the positionally exchanged UTP clearly shows an increase in a resonance 0.015 ppm upfield relative to the position for the α-phosphoryl group of the starting material. The NMR spectrum of the equilibrium reaction mixture (produced in the absence of any added pyrophosphatase) is shown in Figure 1C. The experimental ratio of the two sets of resonances for the α-P is 1:3.2. This ratio is consistent only with the complete interconversion of the β- and γ-phosphoryl groups due to the release and rebinding of the PP_i produced in the reaction. The

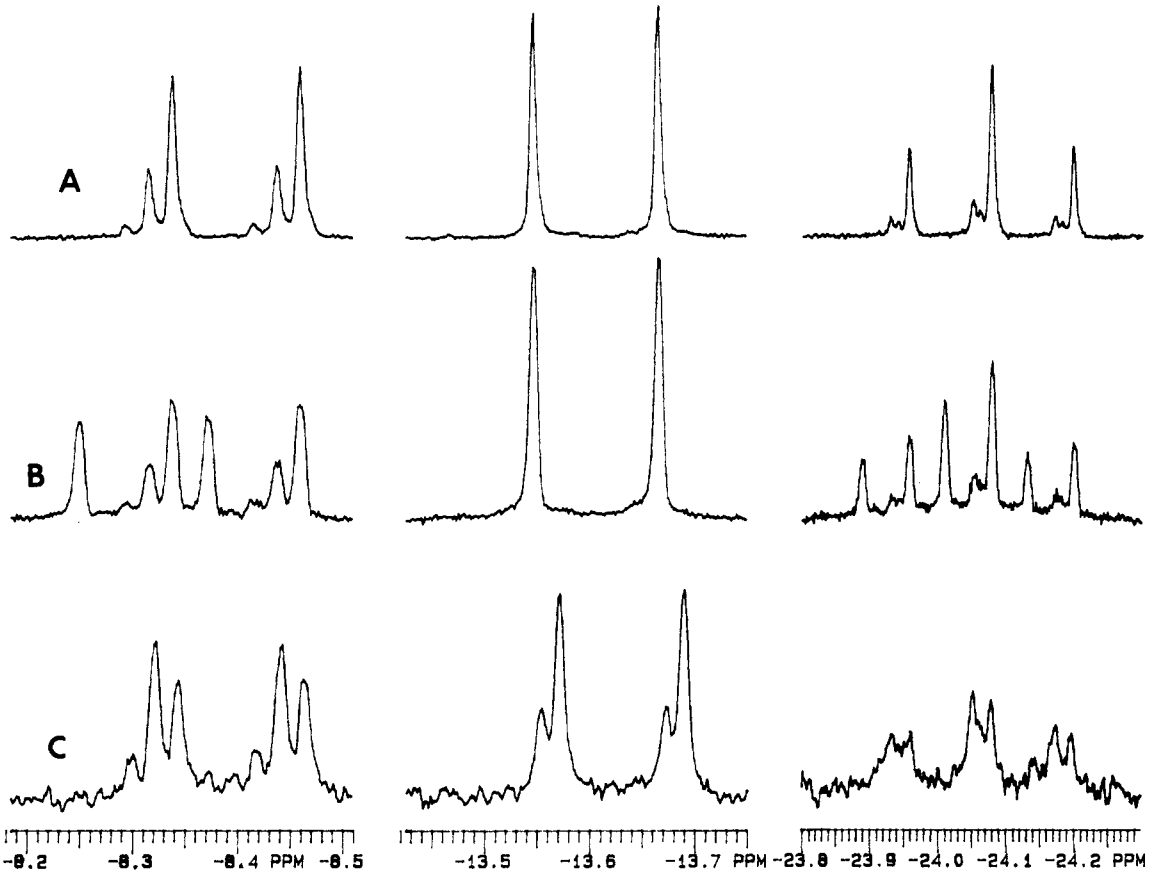

FIGURE 1: (A) ^{31}P NMR spectrum of [β-$^{18}O_2$,$\beta\gamma$-^{18}O,γ-$^{18}O_3$]UTP (I). The α-, β-, and γ-phosphoryl groups are centered at −13.6, −24.08, and −8.41 ppm, respectively. (B) ^{31}P NMR spectrum of a mixture of unlabeled UTP and [β-$^{18}O_2$,$\beta\gamma$-^{18}O,γ-$^{18}O_3$]UTP (I). (C) ^{31}P NMR spectrum of [$\alpha\beta$-^{18}O,β-^{18}O,$\beta\gamma$-^{18}O,γ-$^{18}O_3$]UTP (II) and [β-$^{18}O_2$,$\beta\gamma$-^{18}O,γ-$^{18}O_3$]UTP (I) isolated from a PIX reaction that proceeded to equilibrium.

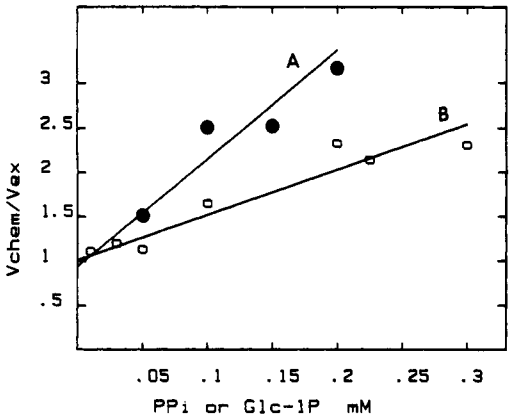

FIGURE 2: Plot of the ratio of the net chemical turnover rate and the positional isotope exchange rate (v_{chem}/v_{ex}) as a function of the concentration of added glucose-1-P (○) or PP_i (●).

Scheme III

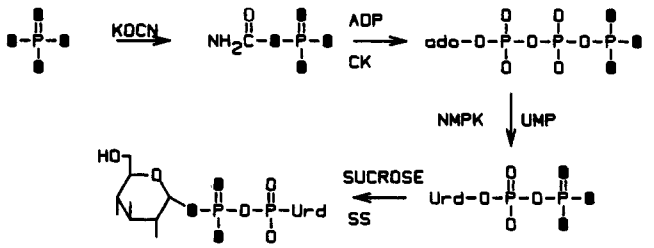

observed ratio of peak heights for the γ-P is 1:3.6:2.5 compared with the calculated value of 1:3.6:2.3.

The partitioning of the EPQ complex in the UDP-glucose pyrophosphorylase reaction has been determined by measuring the rate of positional isotope exchange of an oxygen-18 from a β-nonbridge position to the α,β-bridge position relative to the rate for net product formation. The reactions were carried out in the presence of a large excess of inorganic pyrophosphatase to ensure that once pyrophosphate dissociated from the active site it would be rapidly hydrolyzed. A plot of the positional isotope exchange rate relative to the net chemical turnover vs. the concentration of glucose 1-phosphate is seen in Figure 2. The PIX reactions were also conducted at 1.0 and 10 mM glucose-1-P, but the exchange rate was suppressed far below the detection limits of the NMR measurement. The maximal ratio of rates at zero glucose-1-P (R_1) is 1.0 ± 0.1, and the concentration of glucose-1-P which increases this ratio by a factor of 2 (B_x) is 0.20 ± 0.04 mM. There were no significant changes in the ratio of the peak heights for the γ-P. This would indicate that the β- and γ-phosphoryl groups of the pyrophosphate are unable to interconvert when bound to the active site as has been seen with Val- and Met-tRNA synthetases (Smith & Cohn, 1981).

The strategy for preparing oxygen-18-labeled UDP-glucose (III) is shown in Scheme III. The intermediate synthesis of the [β-$^{18}O_3$]UDP is similar to that described previously for labeled UTP. In the final step, [β-$^{18}O_3$]UDP-glucose is formed from the labeled UDP and sucrose in a reaction catalyzed by sucrose synthetase from wheat germ. The ^{31}P NMR integration of the separate resonances for the β-P of the labeled UDP-glucose indicates an oxygen-18 incorporation of 90%. A NMR spectrum of the final product is shown in Figure 3A.

The incorporation of oxygen-18 into the β-P of UDP-glucose is clearly observed by mixing unlabeled and labeled UDP-glucose as indicated in the ^{31}P NMR spectrum in Figure 3B. The total upfield chemical shift induced by the three atoms of oxygen-18 that are directly attached to the β-P is 0.071 ppm. When UDP-glucose pyrophosphorylase is incubated with [β-$^{18}O_3$]UDP-glucose and PP_i, the β-nonbridge oxygen-18 atoms can exchange with the oxygen-16 atom of the α,β-bridge position. Shown in Figure 3C is the ^{31}P NMR spectrum of the equilibrium mixture. A new resonance is observed for the α-P that is 0.016 ppm upfield from the unlabeled position. This represents the isotopic chemical shift induced by the oxygen-18 in the α,β-bridge position. In the equilibrium mixture, the β-P shows a downfield chemical shift of 0.013 ppm. This value represents the difference in the induced isotopic chemical shift between the β-nonbridge and the α,β-bridge oxygen. Therefore, the isotopic chemical shifts induced by each of the β-nonbridge oxygens can be calculated as 0.029 ppm. The calculated isotopic chemical shift for the anomeric oxygen is 0.013 ppm [0.071 − 2(0.029)]. This agrees well with the results of Singh et al. (1987).

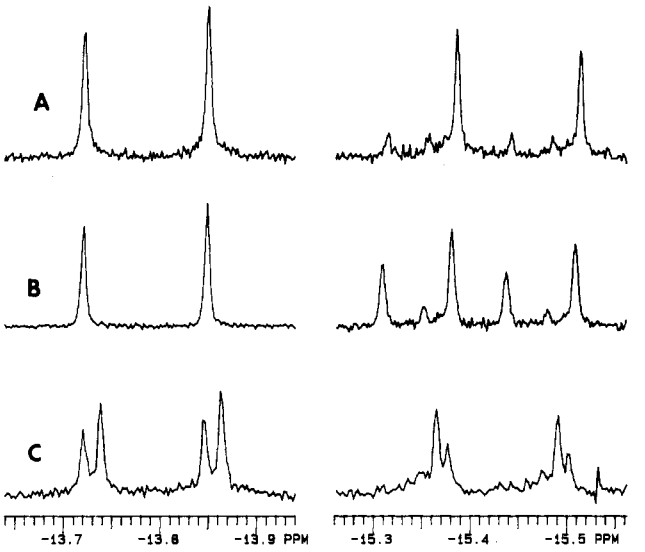

FIGURE 3: (A) ^{31}P NMR spectrum of [β-$^{18}O_3$]UDP-glucose (III). The α-P is centered at −13.8 ppm, and the β-P is centered at −15.45 ppm. (B) ^{31}P NMR spectrum of a mixture of unlabeled UDP-glucose and [β-$^{18}O_3$]UDP-glucose (III). (C) ^{31}P NMR spectrum of [αβ-^{18}O,β-$^{18}O_2$]UDP-glucose (IV) and [β-$^{18}O_3$]UDP-glucose (III) isolated from a PIX reaction that proceeded to equilibrium.

The partitioning of the EAB complex in the UDP-glucose pyrophosphorylase reaction has been measured by determining the rate of positional isotope exchange within UDP-glucose relative to the net rate of product formation. This ratio has been determined as a function of the concentration of PP_i. The addition of phosphoglucomutase and glucose-6-P dehydrogenase to these reaction mixtures was made to prevent glucose-1-P from reassociating with the enzyme after dissociation into the bulk solution. A plot of the positional isotope exchange rate relative to the net chemical turnover as a function of the initial pyrophosphate concentration is shown in Figure 2. No detectable PIX was observed at concentrations greater than 1.0 mM pyrophosphate. The maximal ratio of rates at zero pyrophosphate (R_2) is 0.95 ± 0.24, and the concentration of pyrophosphate that increases this value by 2 (P_x) is 0.08 ± 0.02 mM.

The Michaelis constants for UTP, PP_i, UDP-glucose, and glucose-1-P are listed in Table I along with the values for V_{max} of the forward and reverse reactions. The equilibrium constant for the interconversion of bound substrates and products was determined by incubation of an excess of enzyme with either 20 μM UTP or 17 μM UDP-glucose. A large excess of a 1:1 mixture of PP_i and glucose-1-P was added to force all of the uridine cofactors into an enzyme-bound complex. When the equilibrium condition was approached from the UTP side, the final concentration of UTP was found to be 12 μM. When

Table I: Experimental and Calculated Kinetic Constants for UDP-glucose Pyrophosphorylase[a]

	kinetic constants		
	exptl	calcd	algebraic expression[b]
V_1 (s^{-1})	150	190	$k_5k_7k_9/(k_5k_9 + k_5k_7 + k_6k_9 + k_7k_9)$
K_a (mM)	0.06	0.061	V_1/k_1
K_b (mM)	0.013	0.016	$V_1(k_4k_6 + k_4k_7 + k_5k_7)/k_3k_5k_7$
R_1	1.0	0.82	$k_7(k_4 + k_5)/k_4k_6$
B_x (mM)	0.20	0.21	$k_2(k_4 + k_5)/k_3k_5$
V_2 (s^{-1})	600	525	$k_2k_4k_6/(k_2k_4 + k_2k_5 + k_2k_6 + k_4k_6)$
K_q (mM)	0.25	0.22	V_2/k_{10}
K_p (mM)	0.07	0.18	$V_2(k_4k_6 + k_4k_7 + k_5k_7)/k_4k_6k_8$
R_2	1.0	1.3	$k_4(k_6 + k_7)/k_5k_7$
P_x (mM)	0.08	0.07	$k_9(k_6 + k_7)/k_6k_8$
K'_{eq}	0.70	0.78	k_5/k_6
K_{eq}	0.30	0.33	$k_1k_3k_5k_7k_9/k_2k_4k_6k_8k_{10}$

[a] These values were obtained at pH 7.5 and 25 °C. The maximal velocities were calculated by assuming a tetramer of four equivalent and functioning subunits of M_r 60000 and a specific activity of 150 μmol min^{-1} mg^{-1}. The calculated values were obtained by using the rate constants presented in Table II. [b] The algebraic expressions were derived with Scheme I as a model using the theory of net rate constants of Cleland (1975).

the equilibrium was approached from the UDP-glucose side, the final concentration of UTP at saturating PP_i and glucose-1-P concentrations was found to be 10 μM. The calculated average equilibrium constant for the expression [UDP-glucose][PP_i]/[UTP][glucose-1-P] is 0.7 ± 0.2.

Discussion

Positional Isotope Exchange Inhibition (PIXI). Raushel and Garrard (1984) have previously presented the theory for the enhancement of positional isotope exchange rates by added products in enzyme-catalyzed reactions. The PIXE technique can be effectively used for the determination of enzyme kinetic mechanisms and for the measurement of microscopic rate constants for ligand dissociation from enzyme–product complexes. In this paper, we have derived the algebraic expressions for the effect of varying the concentration of nonlabeled substrate on the rate of positional isotope exchange. These equations have shown that the increase in the concentration of the nonlabeled substrate will lead to a diminution of the positional isotope exchange rate relative to the net rate for substrate turnover. This inhibition of the PIX rate can be used to determine the kinetic mechanism and to obtain quantitative information about the partitioning of enzyme–substrate and enzyme–product complexes.

In ordered kinetic mechanisms, the inhibition of the PIX rate will occur whenever the nonlabeled substrate adds to the enzyme after the labeled substrate. Inhibition occurs because the nonlabeled substrate is able to totally prevent the substrate that can undergo positional isotope exchange from dissociating into the bulk solution. In random kinetic mechanisms, the inhibition is only partial because the nonlabeled substrate can diminish, but not totally prevent, the dissociation of the labeled substrate into solution. Therefore, an analysis of the inhibitory effect by the nonlabeled substrate on the PIX rate can be used to obtain the order of addition of substrates to the enzyme active site.

A quantitative analysis of the inhibition by added substrates on the PIX rates can also be used to measure the partitioning of enzyme–product and enzyme–substrate complexes. Equation 5 predicts that in an ordered kinetic mechanism an increase in the concentration of the nonlabeled substrate will cause a linear increase in the ratio of the net rate for substrate turnover and the rate of positional isotope exchange. The relative PIX rate will be maximal as the concentration of the nonlabeled substrate approaches zero. The value for R_1 thus represents the partitioning of the ternary enzyme–product complex (EPQ). It can easily be shown that the rate constant for the release of the first product from EPQ (k_7) relative to the maximal velocity in the reverse direction (V_2) is greater than or equal to R_1 and thus

$$k_7/V_2 \geq R_1 \tag{10}$$

This same PIX experiment can also provide information on the partitioning of the binary enzyme–substrate complex (EA). A comparison of the amount of B that is needed to reduce the relative PIX rate by a factor of 2 (B_x) and the Michaelis constant for B (K_b) can be used to measure the rate constant for the dissociation of A from the EA complex (k_2) relative to the maximal velocity of the forward reaction (V_1):

$$k_2/V_1 = (B_x/K_b)(R_1 + 1)/R_1 \tag{11}$$

Therefore, a quantitative analysis of the inhibition of the PIX rate by the nonlabeled substrate can permit the measurement of the rate constant for the dissociation of A from EA (k_2) and the lower limit for the dissociation of P from EPQ (k_7). If an independent PIX reaction can be measured in the reverse direction, then the partitioning of the remaining two complexes, EQ and EAB, will be known as will the relative values for k_9 and k_4. Furthermore, if the values from the PIX experiments (R_1, R_2, B_x, and P_x) are combined with the kinetic constants for the steady-state experiments (V_1, V_2, K_a, K_b, K_p, and K_q) and the thermodynamic parameter, K_{eq}, then it should be possible to provide good estimates for all 10 microscopic rate constants in the minimal scheme for an ordered kinetic mechanism. There are now more independent expressions for measurable constants than there are individual rate constants.

There are a number of conditions where the analysis of the PIX rates will be unable to provide qualitative or quantitative information about an enzyme mechanism. If the release of products from the ternary enzyme complexes (either EAB or EPQ) is very much faster than the interconversion of these same complexes, then no PIX will be observed. This is because product dissociation is much faster than resynthesis of the initial substrates, and thus no PIX can ever be observed. Therefore, if the ligands (either substrate or products) are very "nonsticky", then the relative PIX rate will be too slow to measure with the available techniques. The problem with slow PIX reactions in systems where the isotopically labeled substrates are constantly being depleted is that the chemical reaction must be allowed to go almost to completion in order for a significant fraction of the isotope label to be positionally exchanged.

The other problem is one of restricted bond rotation. If the rate of bond rotation is slower than the rate for the interconversion of enzyme complexes, then the quantitative analysis of the PIX experiments will be invalid. In most systems, this should be of no problem since there is little barrier to phosphoryl group rotation ($\sim 10^{12}$ s^{-1}, Engelke, 1973). However, the rate of rotation when these groups are bound to the enzyme is unknown.

UDP-glucose Pyrophosphorylase. The ratio of the PIX rate and the rate of net chemical turnover was measured as a function of the concentration of the nonlabeled substrate for both the forward and reverse reactions catalyzed by UDP-glucose pyrophosphorylase. This reaction is ideal for analysis by PIX techniques because a different exchange reaction can be measured in both directions. Moreover, the kinetic mechanism is ordered, and the maximal velocities in the forward and reverse direction are within a factor of 10 of each other. The ordered kinetic mechanism reduces to 10 the

Table II: Calculated Rate Constants for UDP-glucose Pyrophosphorylase Reaction[a]

$k_1 = 3.2 \times 10^6\ M^{-1}\ s^{-1}$	$k_6 = 3.0 \times 10^4\ s^{-1}$
$k_2 = 5.6 \times 10^3\ s^{-1}$	$k_7 = 1.1 \times 10^3\ s^{-1}$
$k_3 = 2.9 \times 10^7\ M^{-1}\ s^{-1}$	$k_8 = 5.3 \times 10^6\ M^{-1}\ s^{-1}$
$k_4 = 1.1 \times 10^3\ s^{-1}$	$k_9 = 3.4 \times 10^2\ s^{-1}$
$k_5 = 2.3 \times 10^4\ s^{-1}$	$k_{10} = 2.4 \times 10^6\ M^{-1}\ s^{-1}$

[a] See Scheme I for definition of mechanism.

minimum number of rate constants to consider for a 2-substrate/2-product reaction. The near-equivalent V_{max} values suggest that the individual rate constants that govern the forward and reverse reaction velocities will be about the same order of magnitude.

The plots of the relative PIX rates as a function of the concentration of pyrophosphate and glucose-1-P shown in Figure 2 clearly indicate that UDP-glucose pyrophosphorylase has an ordered kinetic mechanism in both the forward and reverse directions. These results are supported by the steady-state kinetic analysis of this reaction by Tsuboi et al. (1969). Since a PIX reaction is measurable in both the forward and reverse directions, the interconversion of the central complexes (E·UTP·Glc-1-P and E·UDP-Glc·PP_i) must be fast relative to the rates of dissociation of glucose-1-P and pyrophosphate from these ternary complexes. Otherwise, the products would be dissociating into solution much faster than the positional isotope exchange reaction could occur.

The positional isotope exchange data, the steady-state kinetic constants, and the external and internal equilibrium constants have been used to obtain values for all 10 rate constants of the minimal model presented in Scheme I. In this analysis, there are 12 independent measurements and 10 constants to be determined. The values for the rate constants, k_1 through k_{10}, obtained in this manner are listed in Table II. The calculated rate constants have been substituted back into the algebraic expressions for all 12 experimental constants in order to get an indication for how well the calculated values compare with the experimentally determined values. These comparisons are presented in Table I and are generally quite good. The only exception is the Michaelis constant for pyrophosphate which differs only by a factor of about 2.

Examination of the calculated rate constants presented in Table II provides an indication of which steps in the mechanism are the slowest. In the forward direction, the release of UDP-glucose is 3 times slower than the release of pyrophosphate. In the reverse direction, the release of glucose-1-P is 5 times slower than the release of UTP. It should be noted, however, that this analysis is based on a minimal scheme for an ordered mechanism. Any conformational steps that may occur have been incorporated into the binding and dissociation steps.

Summary

The inhibition of PIX rates by nonlabeled substrates can be used to obtain qualitative and quantitative information about enzyme-catalyzed reaction mechanisms. Application of this technique to the reaction catalyzed by UDP-glucose pyrophosphorylase has indicated that the release of UDP-glucose and the release of glucose-1-P are the slowest steps in the forward and reverse reactions, respectively.

References

Albery, J., & Knowles, J. (1976) *Biochemistry 15*, 5627–5631.
Albery, J., & Knowles, J. (1986) *Biochemistry 25*, 2572–2577.
Cleland, W. W. (1975) *Biochemistry 14*, 3220–3224.
Cohn, M. (1982) *Annu. Rev. Biophys. Bioeng. 11*, 23–42.
Cohn, M., & Hu, A. (1980) *J. Am. Chem. Soc. 102*, 913–916.
Cook, P. F., & Cleland, W. W. (1981) *Biochemistry 20*, 1790–1796.
DeBrosse, C., & Villafranca, J. J. (1983) in *Magnetic Resonance in Biology* (Cohen, S., Ed.) pp 1–52, Wiley, New York.
Engelke, S. Z. (1973) Ph.D. Thesis, University of New Mexico.
Hassett, A., Blattler, W., & Knowles, J. R. (1982) *Biochemistry 21*, 6335–6340.
Litwin, S., & Wimmer, M. J. (1979) *J. Biol. Chem. 254*, 1859.
Midelfort, C. F., & Rose, I. A. (1976) *J. Biol. Chem. 251*, 5881–5887.
Raushel, F. M., & Villafranca, J. J. (1980) *Biochemistry 19*, 3170–3174.
Raushel, F. M., & Garrard, L. J. (1984) *Biochemistry 23*, 1791–1795.
Riseley, J. M., & Van Etten, R. L. (1978) *J. Labelled Compd. Radiopharm. 15*, 533–538.
Rose, I. A., O'Connell, E. L., Litwin, S., & Bar Tana, J. (1974) *J. Biol. Chem. 16*, 5163–5168.
Sheu, K. R., & Frey, P. A. (1978) *J. Biol. Chem. 253*, 3378–3383.
Singh, A. N., Hester, L. S., & Raushel, F. M. (1987) *J. Biol. Chem. 262*, 2554–2557.
Smith, L. T., & Cohn, M. (1981) *Biochemistry 20*, 385–391.
Tsuboi, K. K., Fukunaga, K., & Petricciani, J. C. (1969) *J. Biol. Chem. 244*, 1008–1015.
von der Saal, W., Anderson, P. M., & Villafranca, J. J. (1985) *J. Biol. Chem. 260*, 14993–14997.